Rydberg states of DABCO.cntdot.Krn clusters

ARTICLE *in* THE JOURNAL OF PHYSICAL CHEMISTRY · JULY 1993

Impact Factor: 2.78 · DOI: 10.1021/j100130a011

3 AUTHORS, INCLUDING:

Uzi Even
Tel Aviv University
176 PUBLICATIONS **5,514** CITATIONS
SEE PROFILE

A. Gedanken
Bar Ilan University
362 PUBLICATIONS **11,476** CITATIONS
SEE PROFILE

Rydberg States of DABCO·Kr_n Clusters

D. Bahatt* and U. Even*

School of Chemistry, Sackler Faculty of Exact Sciences, Tel-Aviv University, Tel Aviv 69978, Israel

A. Gedanken*

Department of Chemistry, Bar-Ilan University, Ramat-Gan 52900, Israel

Received: December 29, 1992; In Final Form: April 2, 1993

The spectroscopy of DABCO·Kr_n (1,4-diazabicyclo[2.2.2]octane) clusters was investigated using a two-color mass-selected ionization process. The transition from the ground state to the first excited state of DABCO (which is already a Rydberg state) is one photon forbidden and was the object of our studies. In the mixed cluster, this transition becomes allowed due to the reduced symmetry and its origin was detected in DABCO·Kr_n clusters for $n = 1$–3. Structural isomers of these clusters were identified and characterized by the spectral shifts of both the $S_0 \rightarrow S_1$ and the $S_0 \rightarrow$ IP transitions using combination rules. The blue shifts which were observed for the S_1 Rydberg state differ from previous reports of a red shift for a valence state undergoing the clustering process.

Introduction

The spectroscopy of van der Waals heteroclusters has recently been the subject of many investigations.[1] The properties of the heterocluster M·RB_n, where M is a polyatomic molecule and RG a rare-gas atom, were probed through the excited states of the "guest" molecule. The excited states chosen for these studies were always valence states, and most of the published work has been carried out on the S_1 state of aromatic molecules. The energetics of the heterocluster has been obtained from the spectral shift of the $S_0 \rightarrow S_1$ excitation of the heterocluster relative to the origin of the bare molecule. The dynamics was derived from the radiative decay of this excited state in comparison with that of the bare guest molecule.

The current study was aimed at probing the energetics of Rydberg states of heteroclusters and comparing spectral properties such as the spectral shifts with those reported for valence states.[2] We chose DABCO (1,4-diazabicyclo[2.2.2]octane), shown in Figure 1, as the subject of this investigation.

The reason for choosing DABCO is as follows: in DABCO, as in other amines, all the detected excited states in one-photon absorption are characterized as Rydberg transitions.[3] The $S_0 \rightarrow S_1$ (n(N) $\rightarrow$ 3s) transition is electric dipole forbidden in one photon (belonging to the D_{3h} symmetry group) and has therefore a relatively long lifetime ($\sim$1 μs).[4] Its long lifetime has made this transition a favorable candidate for two-color experiments in which the S_1 state served as an intermediate state.[5] The S_1 origin in DABCO is located in the near-UV (2794.6 Å = 35 783 cm^{-1})[6,7] which makes it easily accessible for laser excitation, whereas most of the first Rydberg transitions in polyatomic molecules are found in the vacuum UV.[4] The difficulty of reaching the origin of the S_1 state in DABCO by a one-photon process is overcome by exciting the molecule to one of its false origins.[6,7] Another option would be to reach the true origin via a two-photon excitation.

In DABCO·RG_n heteroclusters, the symmetry "problem" is overcome by the RG atoms which can break the symmetry. From this point of view, DABCO again is a good candidate molecule, since it was found to be an efficient clustering center.[7b]

Interpretation of the cluster structure is facilitated by using combination rules.[1b] The spectral shifts can be expressed approximately as a cumulative contribution from the individual rare-gas atoms. The application of the combination rules allows for a self-consistent assignment of isomer structures.

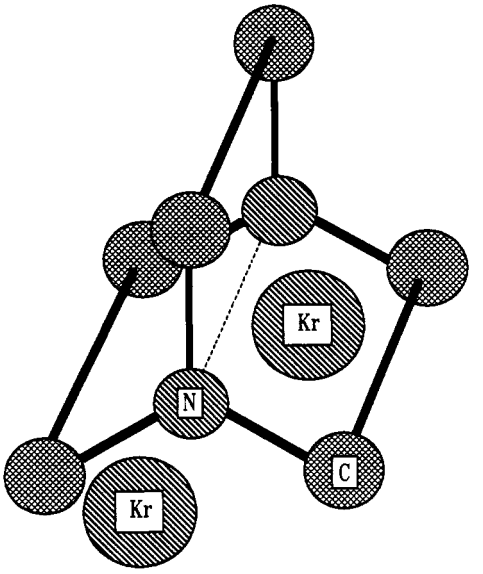

Figure 1. Schematic representation of DABCO and the possible sites for the Kr atoms (equatorial and polar).

Experimental Section

The experimental system is schematically presented in Figure 2. The molecular beam was generated in a three-chamber differentially pumped vacuum system. The first chamber contained a fast (100-μs) magnetically actuated pulsed valve operated at 10–15 Hz. This valve can be heated to 450 °C. The valve was fitted with a conical nozzle (ϕ = 0.5 mm, 30° full angle, 2 mm long).[8] The short opening time and the conical-shaped expansion reduced the required pumping seed throughput (to less than 0.1 L·Torr/s) even at stagnation pressures of 3 atm. We found that a carrier gas mixture of 30% He in Ne (Ne70) produced the best cooling. The expansion mixture contained the carrier gas, 10% Kr as the clustering agent, and 0.1–1 Torr of DABCO molecules (obtained by heating the nozzle to 100 °C).

The molecular beam was skimmed and passed to the second chamber containing a Wiley–McLaren time-of-flight mass spectrometer[9] and a magnetic-bottle ZEKE (zero kinetic energy) electron spectrometer.[10] To skim the intense beam, we used a skimmer with a large opening (ϕ = 4 mm) of a simple conical shape (50° full angle) made of electroformed nickel. The pressure

0022-3654/93/2097-7189$04.00/0

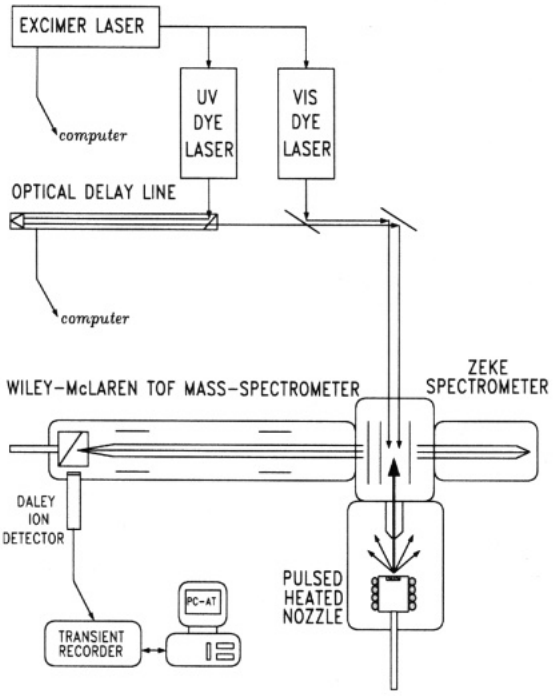

Figure 2. Schematic representation of the experimental system.

at the spectrometers was maintained at 10^{-6} Torr. For detecting the mass-selected ions, we used a Daley detector[11] with high sensitivity for large masses. A mass resolution of $M/\Delta M \approx 500$ was achieved (up to masses of 2500 amu) with a 1.3-m flight tube perpendicular to the molecular beam direction. ZEKE electrons were produced by a short (~10-ns), 5 V/cm field ionizing pulse and detetected with a two-stage microchannel plate detector (Hamamatsu F-1552). A typical electron kinetic energy resolution of ~2 cm^{-1} was easily achieved with a short (300-mm) flight tube.

The molecular beam was probed by resonant two-color two-photon excitation. One (UV) photon was tuned to the $S_0 \rightarrow S_1$ ($v' = 0$ or 1) transition in DABCO or scanned along this transition in the DABCO·Kr_n clusters. The other (visible) photon was scanned either along the Rydberg series of the bare molecule up to the series limit (4540–4990 Å), resulting in a highly excited Rydberg state which were then field ionized to produce ZEKE electrons, or along the ionization threshold of the cluster, resulting in an ion of the interrogated species. The technique of resonant two-color two-photon ionization (R2C2PI) coupled with high-resolution mass selection was found to discriminate against interference from various species found in the beam. These can be impurities or thermal decomposition or photodecomposition products of the bare molecule. More important, this method can discriminate against fragmentation of clusters due to the excitation. We found this method superior compared to laser-induced fluorescence or REMPI.

An excimer laser (Lambda Physik 150MSC) was used for pumping two dye lasers (Lambda Physik FL2002) simultaneously. The two slightly focused (2-mm beam waist) laser beams, overlapping in the ionization/excitation region of the spectrometers, were aligned for counterpropagation with the molecular beam, resulting in a long ionization/excitation cylinder (limited by the ion/electron collection optics to 10-mm length). Pulse energies of 0.1 mJ for the UV photon and 1 mJ for the visible (at a laser duration of 7 ns) were sufficient to produce 10^3 ions/pulse of the parent species. The laser peak power for the UV pulse was carefully adjusted (250 kW/cm^2) so that saturation effects and R2PI were negligible.

Results

1. Highly Excited Rydberg States in DABCO. The ZEKE spectra of the $S_1(v' = 1) \rightarrow$ Rydberg series transition of DABCO

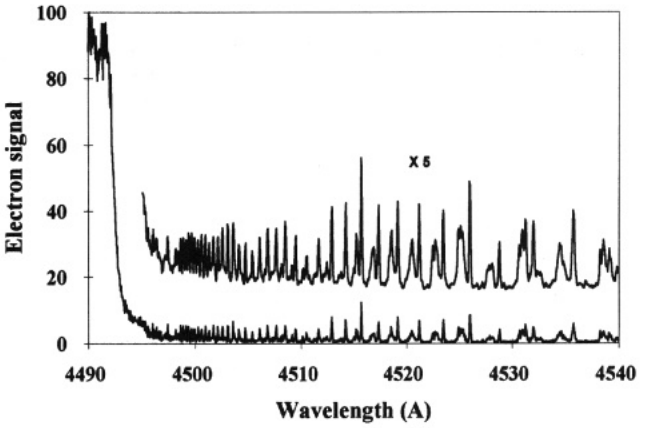

Figure 3. ZEKE spectrum of the $S_1(v' = 1007\ cm^{-1}) \rightarrow$ Rydberg series of DABCO. The first photon was tuned to the 1007-cm^{-1} vibrational level in the 3s state. The second photon was scanned along the Rydberg series.

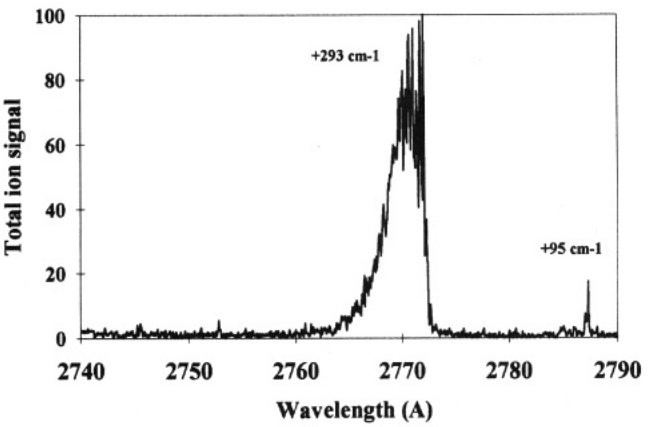

Figure 4. Total ion spectrum of the $S_0(v = 0) \rightarrow S_1(v' = 0)$ transition of DABCO·Kr_1. The abscissa represents the excitation wavelength. The second photon was set to above the threshold ionization.

are presented in Figure 3. By exciting the 1007-cm^{-1} C–H stretching mode[6] in the S_1 state, the full series of high Rydberg states (58 816–59 037 cm^{-1}) is revealed and detected because of the large Franck–Condon factors between the involved states.

Our results agree with the previous results of Ito et al.[7] We observe the same three Rydberg series with quantum defects of $\delta = 0.41(\pm 0.01)$, $0.23(\pm 0.02)$, and $0.05(\pm 0.01)$. These series converge to a vertical ionization potential of 59 046 cm^{-1}. In our spectrum, we detect extended Rydberg series up to $n_{max} \approx 45$ (as compared to Ito et al. where $n_{max} = 35$).

2. Low-Lying Rydberg States in DABCO·Kr_n Clusters. The total ion spectra of the one-photon $S_0(v = 0) \rightarrow S_1(v' = 0)$ transition of DABCO·Kr_n (n = 1–3) clusters are presented in Figures 4–6. No clusters with He or Ne were found, probably due to low binding energies and fragmentation upon excitation.

For DABCO·Kr_1, two spectral features were observed. The first is blue shifted relative to the 0–0 transition of the bare molecule by 95 cm^{-1} (35 878 cm^{-1}). This band appears as a weak transition and a short (three lines) vibrational progression with ~2-cm^{-1} spacing. The ionization potential of this feature is red shifted by 156 cm^{-1} relative to that of the bare molecule. The second much stronger feature is blue shifted by 293 cm^{-1} (36 076 cm^{-1}) and appears as a long (about 20 lines) vibrational progression with 4.4-cm^{-1} spacing. The ionization potential of this feature is blue shifted by 68 cm^{-1} relative to that of the bare molecule. This progression is unusual and indicates low binding energies and shifted potential surfaces.

For DABCO·Kr_2 and DABCO·Kr_3, intense spectral lines appear at linear combinations of the spectral shifts observed in the DABCO·Kr_1 cluster. Of these strong lines, some appear as narrow bands and some as broad bands.

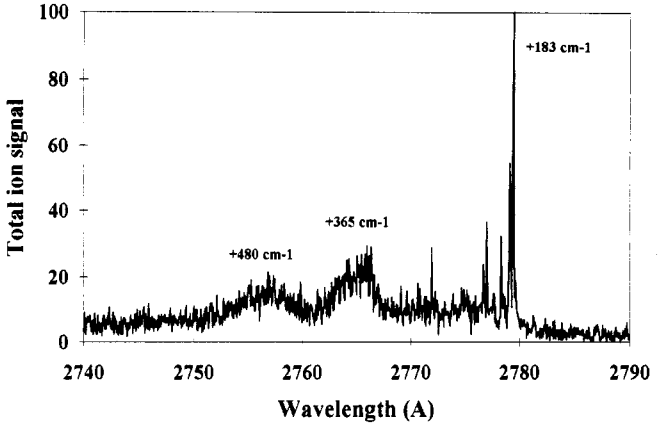

Figure 5. Total ion spectrum of the $S_0(v = 0) \rightarrow S_1(v' = 0)$ transition of DABCO·Kr_2. The abscissa represents the excitation wavelength. The second photon was set to above the threshold ionization.

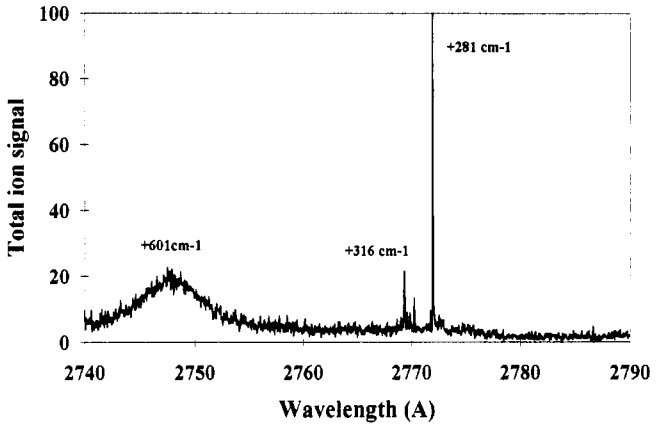

Figure 6. Total ion spectrum of the $S_0(v = 0) \rightarrow S_1(v' = 0)$ transition of DABCO·Kr_3. The abscissa represents the excitation wavelength. The second photon was set to above the threshold ionization.

For DABCO·Kr_2, the main spectral features are blue shifted by +183, +365, and +480 cm^{-1} relative to the bare molecule 0–0 transition. The ionization potential of the first two features is red shifted by 284 and 29 cm^{-1} (respectively) relative to that of the bare molecule.

For DABCO·Kr_3, the main spectral features are blue shifted by +281, 316, and +601 cm^{-1}. The ionization potentials of these features are red shifted by 428, 440, and 164 cm^{-1} (respectively) relative to that of the bare molecule.

The observed large blue spectral shifts of the $S_0 \rightarrow S_1$ transition are unusual. This type of behavior is not commonly found in the case of excited valence states of aromatic molecules embedded in Kr clusters (where red shifts of ~80 cm^{-1} are observed for Kr). These shifts will be interpreted as the effect of rare-gas atoms on the 3s Rydberg state of DABCO.

The spectral shifts and the ionization thresholds of the DABCO·Kr_n clusters are summarized in Table I.

Discussion

The spectral shifts and intensities of the spectral features in the DABCO·Kr_n (n = 1–3) clusters are related to different possible coexisting isomers of the cluster systems.

1. DABCO·Kr_1. Spectral Features and Isomeric Forms. A Kr atom can cause a red or blue shift of electronic transitions, depending on the character of the involved electronic states of the bare molecule and the nature of the intermolecular interaction. As mentioned above, valence electronic states in aromatic molecules are commonly red shifted by RG atoms,[3] while Rydberg electronic states in amines are blue shifted.[4] The interpretation of the cluster spectrum strongly depends on the sign and magnitude of the spectral shifts and is necessary for the determination of the cluster structure.

TABLE I: Spectral Shifts and Ionization Thresholds of the Main Features in the Spectra of the DABCO·Kr_n Clusters[a]

n	isomer	$S_0 \rightarrow S_1$, cm^{-1}	$S_1 \rightarrow$ IP, cm^{-1}	ionization pot., cm^{-1}	ΔI_p, cm^{-1}
0		35 783	22 249	58 032	0
1	1E	+95	21 998	57 876	−156
	1P	+293	22 024	58 100	+68
2	2E	+183	21 782	57 748	−284
	1E1P	+365	21 855	58 003	−29
		+480			
3	3E	+281	21 540	57 604	−428
	3E (?)	+316	21 493	57 592	−440
	2P1E	+601	21 484	57 868	−164

[a] Ionization potential is taken at the onset wavelength of the ion signal. (e-equatorial isomer, p-polar isomer).

We shall attempt to interpret the cluster spectrum, using these different mechanisms, in order to check their validity.

The first excited state of DABCO is generated from the promotion of a nonbonding electron on the nitrogen atom to a 3s Rydberg orbital. This excited state belongs to the $^1A_1'$ symmetry group, and the transition from the ground state is one-photon forbidden and two-photon allowed. This is the reason that in the excitation fluorescence spectrum of DABCO the origin is absent, and instead four false origins of e′ symmetry are detected. The false origins were observed at 0–0 +499, 0–0 +823, 0–0 +921, and 0–0 +1007 cm^{-1}.[6,7]

In assigning the spectrum of DABCO·Kr_1, we can try to associate the 35 878-cm^{-1} and the 36 076-cm^{-1} bands of DABCO·Kr_1 with the first false origin of the bare molecule, namely, +449 cm^{-1}, which appears at 36 232 cm^{-1}. The rationalization for this attempt is the fact that the bands in DABCO·Kr_1 are detected as one-photon transitions and are therefore assumed to be false origins similar to those of the bare molecule. Since the 449-cm^{-1} origin is the lowest of the four false origins, it is the closest to the DABCO·Kr_1 bands, and the shifts that will be required to relate those bands are the smallest. We reject, however, this approach due to the following reasons:

(1) If the bands in DABCO·Kr_1 are related to the 0–0 +449-cm^{-1} line, they are red shifted compared to this false origin by 156 and 354 cm^{-1}. These red shifts are large compared with the 80-cm^{-1} shifts found for Kr clusters on aromatic molecules.[12]

(2) The addition of the Kr atom reduces the symmetry of DABCO (D_{3h}) and allows a one-photon transition to the 3s Rydberg. Thus, the true 0–0 transition of the cluster should be observed.

Another possibility for the assignment of the +95-cm^{-1} and the +293-cm^{-1} bands is to relate them to vibrations that are active in DABCO·Kr_1 and nonactive in the bare molecule. Such a vibration could be ν_{13} (a_1'' symmetry) whose frequency in the excited state is 99 cm^{-1}.[6,7] This idea is also rejected due to symmetry arguments. We cannot foresee a situation in DABCO·Kr_1 where the origin is absent, whereas a vibronic transition with $^1A_1''(=A_1' \otimes a_1'')$ symmetry is revealed. The transition to a $^1A_1''$ state is forbidden not only in the D_{3h} group but also in the C_{2v} and C_{3v} symmetry groups describing DABCO·Kr_1 (it is reduced to a forbidden A_2 state).

On the basis of these arguments, we relate the 35 878-cm^{-1} and 36 076-cm^{-1} bands of DABCO·Kr_1 to the true origin of DABCO at 35 783 cm^{-1}. These bands are thus blue shifted by +95 and +293 cm^{-1}, respectively. The two bands are assigned as origins of transitions to the 3s Rydberg state in two different isomers. The first, associated with +95-cm^{-1} shift, is described as an isomer where the Kr atom rests between the N–CH_2–CH_2–N plans (equatorial position). The second isomer, related to the +293-cm^{-1} shift, represents an isomer in which the Kr atom is found adjacent to the nitrogen atom and along the N–N axis (polar position).

What is the origin of a blue shift? It can be explained as follows: In the S_0 (ground) electronic state, the lone pair electrons are concentrateed near the nitrogen atom to a larger degree compared to the excited state. Thus, the overlap with the Kr atom (lying near the nitrogen) and the stabilization energy are larger in the ground state. This is only true if the attractive forces between the Kr and the molecule dominate the repulsive forces. If this is the case, a blue shift of the transition is expected. Following this explanation, the position of the Kr atom, relative to the nitrogen atoms, should strongly affect the magnitude of the blue shift. On the basis of this conclusion, we can assign the spectral features of the cluster to two different structural isomers.

If the Kr atom lies in the equatorial position (on the σ_h mirror plane), it is far from the lone pair electrons of the nitrogens participating in the $S_0 \rightarrow S_1$ transition and slightly effects its probability. The symmetry of the molecule is reduced to C_{2v} symmetry, and the $^1A_1'$ state of the D_{3h} symmetry group becomes an $^1A_1$ state to which a one-photon transition from the ground state is allowed. This isomer appears in the spectrum as a weak transition with a narrow line, at +95 cm^{-1} relative to the 0–0 transition of the bare molecule.

If the Kr atom lies in the polar position, it is close to the lone pair electrons and strongly effects the transition probability. In this isomer, the σ_h mirror plane (perpendicular to the C_3 axis) does not exist and the D_{3h} symmetry is reduced to C_{3v} symmetry. The 3s Rydberg state will have an $^1A_1$ symmetry to which the transition from the ground state is allowed. This isomer is characterized by a larger oscillator strength and a larger blue shift as compared to the other isomer. This isomer appears in the spectrum as a long and strong progression at +293 cm^{-1}. Similar blue shifts were found by Meijer et al. in the triphenylamine·(Ar,Kr,Xe) clusters.[13]

The equatorial isomer belongs to the C_{2v} symmetry group, while the polar isomer belongs to the C_{3v} symmetry group. The expected higher intensity associated with the C_{2v} group was not found. Although the D_{3h} symmetry is reduced to the C_{3v} or C_{2v} symmetries and the one-photon transitions become allowed, the oscillator strength of the transitions can still be small. For example, in ABCO (1-azabicyclo[2.2.2]octane), which is very similar to DABCO and belongs to the C_{3v} symmetry group, the 0–0 transition is allowed and the molar extinction coefficient (ϵ) is only ~750.[6a]

The ionization thresholds of these spectral features differ both in sign and in magnitude, thus supporting our conclusion of coexisting structural isomers. The strong perturbation of the lone pair electrons in the polar isomer results in a surprsingly small and blue-shifted threshold. In the equatorial isomer, this perturbation is smaller and the common large red shift is found.

Potential Curves: Force Constants. The long vibrational progression, of very small and constant 4.4-cm^{-1} spacing (Figure 4), appearing in the +293-cm^{-1} isomer, is not typical for this type of heterogeneous clusters. The mean spacing between the progression lines is ϖ = 4.4 cm^{-1}. The structure of this spectral line resembles a transition between two displaced harmonic-oscillator potential curves. According to Siebrand,[14] we can calculate the force constant k and the displacement ΔQ in the excited state:

$$k\ (\mathrm{N/m}) = m\omega^2 = 4\pi^2 mc^2\varpi^2 = 5.9 \times 10^{-5} m\varpi^2 \quad (1)$$

$$\Delta Q\ (\mathrm{A}) = [2h\gamma/m\omega]^{1/2} = [h\gamma/\pi mc\varpi]^{1/2} = 8.21[\gamma/m\varpi]^{1/2} \quad (2)$$

$$\gamma = k(\Delta Q)^2/2h\omega \quad (3)$$

where m is given in amu and ϖ in cm^{-1}.

By fitting γ and n to the observed transitions, we obtain the values of γ = 14.5 and $n_{initial}$ = 7. From this result, the displacement and force constant of the excited state were calculated to be 1.6 Å and 0.1 N/m, respectively. The mass m is taken as the mass of the Kr atom. This is a fairly good approximation, because of the large difference between the DABCO intramolecular vibration frequencies (449 cm^{-1}) and the Kr–DABCO intermolecular vibration frequencies (4.4 cm^{-1}). Using the results for $n_{initial}$, the total number of observed lines, and ϖ, we can only estimate a lower limit for the depth of the potential curve of the excited state to be ~100 cm^{-1}.

This result indicates that the Kr atom is pushed to a considerable distance from the nitrogen atom and the bonding becomes very "soft" in the excited electronic state. The most intriguing result of the above analysis is the 1.6-Å displacement of the excited-state potential curve. The magnitude of the displacement seems to be unreasonably large and to our knowledge was never observed in similar systems (compare to ref 13).

We conclude that explaining the long progression of 4.4-cm^{-1} spacing by using only one active progression is highly unreasonable. Another explanation would be that two or more vibrations are active in the spectrum. This would lead us to assume, in the case of two active vibrations, that there are two series of bands each with a ~10-cm^{-1} spacing.

The soft vibrations in this progression originate from a wagging motion of the Kr atom relative to the C_3 axis along the N–N bond. Similar modes are found in aromatic systems such as tetracene·Ar_n and tetracene·Kr_n clusters. In those systems, vibrations along the x and y axes of the molecule have the same low energies originating from a weakly bonding potential curve.[15]

A much shorter progression is observed in the +95-cm^{-1} isomer (Figure 4). This progression consists of only three lines, the lowest energy 0–0 line being the strongest. For this progression, an extremely low value of ϖ = 1.97 cm^{-1} is found. Fitting γ and n to the observed transitions result in γ = 1 and $n_{initial}$ = 1. The displacement and force constant in the excited state are found to be 0.64 Å and 0.02 N/m, respectively.

Stability. The relative intensities of the two isomers can be changed by varying the carrier gas pressure but not by changing its Kr concentration. We found that the intensity of the 1P isomer decreases faster by lowering the pressure (increasing the beam temperature). This led us to the conclusion that the 1P isomer is the less stable isomer of the two.

2. DABCO·Kr_2. The second Kr atom can also lie in the equatorial or polar positions. According to the positions of the two Kr atoms, different isomers can be formed and are seen in the spectra (Figure 5). The different isomers will be assigned assuming additive spectral shifts.

The narrow strong spectral feature at +183 cm^{-1} and ionization energy shift of –284 cm^{-1} are assigned as the isomer in which both Kr atoms are equatorial (labeled as 2E). These narrow lines resemble the 1E spectral feature. Their shifts are approximately twice that of the 1E equatorial isomer. Vibrations of 3–9 cm^{-1} can be detected near this origin.

The broad spectral feature at +365 cm^{-1} and its measured ionization energy shift of –29 cm^{-1} are assigned to the 1E1P isomer with one polar and one equatorial Kr atom. This assignment is based on the approximate combination of the respective spectral shifts of the 1E and 1P (n = 1) isomers. This broad line resembles the 1P spectral feature.

A similar broad spectral feature at +480 cm^{-1} is assigned to the 2P isomer, where each Kr atom lies near one of the nitrogen atoms. This assignment is again approximately a combination of the 1P isomer.

3. DABCO·Kr_3. In this cluster, even more combinations of the possible Kr sites occur. In our spectrum, we can easily detect three isomeric forms (see Figure 6).

The first isomer appears as a strong and narrow spectral feature at +281 cm^{-1} with an ionization energy shift of –428 cm^{-1}. We assign this line to a 3E isomer in which each Kr atom lies between

different molecular planes, using the 3×1E combination rule and the 1E isomer values. Again, this narrow line resembles the 1E spectral feature.

The second feature appears at +316 cm^{-1} with an ionization shift of −440 cm^{-1}. We cannot assign this feature to a distinct isomer due to the similarity of spectral shifts to those of the 3E isomer.

The $S_0 \rightarrow S_1$ excitation energy of these two features is similar to the excitation of the 1P isomer. Thus, the +293-cm^{-1} spectral feature of the 1P isomer could have been the result of fragmentation of the $n = 3$ cluster. Nevertheless, the large difference in ionization thresholds (~500 cm^{-1}) rules out this possibility.

The third isomer appears as a broad spectral feature at 601 cm^{-1} with an ionization threshold shift of −164 cm^{-1}. We assign this line to a 2P1E isomer in which two Kr atoms lie near the nitrogen atoms and the third Kr lies between the molecular surfaces. This again is based on combination rules. This broad line resembles the 1P spectral feature.

4. Rydberg States of DABCO in van der Waals Clusters and Solid Rare-Gas Matrices. The spectral shifts of the main features in the spectra of the DABCO·Kr$_n$ (n = 1–3) clusters are summarized in Table I. The blue shifts of the 0–0 transitions increase almost linearly with cluster size for a certain isomeric form (equatorial or polar isomers). In the mixed (equatorial together with polar) isomer clusters, the shifts are a linear combination of the shifts of the different isomers. The fact that the shift per added atom is almost constant indicates that the first three Kr atoms can all lie in the first solvating shell of the cluster, at least in the expansion conditions in our system.

At this stage, we can try to compare the results summarized above for the van der Waals clusters with those reported for impurity states of molecular Rydberg states in solid rare-gas matrices.

It is well documented that the lowest Rydberg state in molecules such as benzene,[16] ethylene,[17] ammonia,[18] methyl iodide,[17] and many others undergoes a large blue shift when the molecule is embedded in a rare-gas solid. The size of the blue shift is matrix dependent, where the largest shifts are obtained for a neon matrix and the smallest for a xenon matrix. The typical blue shifts observed for a Kr matrix are ~4500 cm^{-1}. For CH_3I,[17] a 5255-cm^{-1} shift is reported, while for ethylene[17] the shift is 4390 cm^{-1}. The spectrum of DABCO in rare-gas matrices was not reported. The only amine whose spectrum in rare-gas solid was investigated is ammonia. The blue shift measured for ammonia in an argon matrix at 7470 cm^{-1}.[18] The corresponding shift in a Kr matrix was not reported.

Taking the value of 4500 cm^{-1} as the average blue shift in solid krypton and assuming the additivity of the shifts for the DABCO·Kr$_n$ clusters, we estimate that 40–45 Kr atoms will be required to form the krypton matrix around the DABCO molecule. This value is a rough estimate because it considers only two Kr atoms lying along the N–N axis and all the others as equatorial isomers (2×250 cm^{-1} + 40×95 cm^{-1}). This distance (σ) between adjacent Kr atoms in a krypton matrix is ~4 Å,[19] and the N-C bond length in DABCO is 1.47 Å.[20] Based on a simple geometrical consideration, this assumption is reasonable. An equatorial Kr lying close to the nitrogen can contribute more than 95 cm^{-1} to the blue shift. On the other hand, Kr atoms in the second (and larger) solvation shell contribute less to the total blue shift. Our estimate of 40–45 Kr atoms forming a matrix around the DABCO molecule is comparable with the number of Kr atoms needed to reach saturation of the red shift of valence states of aromatic molecules.[1,2]

Conclusion

Transitions to Rydberg states in DABCO·Kr$_n$ clusters were found to be blue shifted relative to the 0–0 transition of the bare parent molecule. The direction and magnitude (293 cm^{-1} per Kr atom) of the spectral shifts are opposite and much larger than the small red shifts (80 cm^{-1} per Kr atom) found for valence states of aromatic molecules. The blue shifts depend strongly on the position of the Kr atoms in the cluster. Thus, molecular Rydberg states can serve as a probe for isomeric forms of molecule·rare-gas cluster systems. The vibrational structure of the observed transitions allows us to estimate the shape, displacement, and depth of the potential curves of excited Rydberg states in the clusters. The spectral shifts found in DABCOC·Kr$_n$ (n = 1–3) clusters are much smaller than those found for molecular Rydberg states in solid rare gases. A rough estimate is that 40–45 rare-gas atoms are needed to form a Kr matrix around DABCO. The ionization potentials depend on the cluster structure and decrease almost linearly with the cluster size.

Acknowledgment. This work was supported partially by the James Franck Institute for Laser Matter Interaction and by the Israel Academy of Science.

References and Notes

(1) (a) Hermine, P.; Parneix, P.; Coutant, B.; Amar, F. G.; Brechignac, Ph. To be published. (b) Ben-Horn, N.; Bahatt, D.; Even, U.; Jortner, J. *J. Chem. Phys.* **1992**, *97* (9), 6011.

(2) (a) Dao, P. D.; Morgan, S.; Castleman, A. W., Jr. *Chem. Phys. Lett.* **1985**, *113* (2), 219 (b) Perkins, C. L.; Perez, E.; Beck, K. M. *Chem. Phys. Lett.* **1992**, *199* (5), 445. (c) Ben-Horin, N.; Even, U.; Jortner, J. *Chem. Phys. Lett.* **1992**, *188* (1,2), 73. (d) Ben-Horin, N.; Even, U.; Jortner, J. *J. Molec. Struct.* **1992**, *266*, 75.

(3) (a) Avouris, P.; Rossi, A. R. *J. Phys. Chem.* **1981**, *85*, 2340. (b) Hager, J.; Ivanco, M.; Wallace, S. C. *Chem. Phys. Lett.* **1982**, *92* (2), 112. (c) Kawasaki, M.; Kasatani, K.; Sato, H. *J. Chem. Phys.* **1982**, *77* (1), 258. (d) Halpern, A. M.; Ondrechen, M. J.; Ziegler, L. D. *J. Am. Chem. Soc.* **1986**, *108*, 3907.

(4) Halpern, A. M. *Chem. Phys. Lett.* **1970**, *6*, 296.

(5) Fisanick, G. J.; Eichelberger IV, T. S.; Robin, M. B.; Kuebler, N. A. *J. Phys. Chem.* **1983**, *87*, 2240.

(6) (a) Gonohe, N.; Yatsuda, N.; Mikami, N.; Ito, M. *Bull. Chem. Soc. Jpn.* **1982**, *55*, 2796. (b) Consalvo, D.; Oomens, J.; Parker, D. H.; Reuss, J. *Chem. Phys.* **1992**, *163*, 223.

(7) (a) Fujii, M.; Ebata, T.; Mikami, N.; Ito, M. *Chem. Phys. Lett.* **1983**, *101* (6), 578. (b) Shang, Q. Y.; Moreno, P. O.; Li, S.; Bernstein, E. R. *J. Chem. Phys.* **1993**, *98* (3), 1876.

(8) Bahatt, D.; Cheshnovsky, O.; Even, U.; Lavie, N.; Magen, Y. *J. Chem. Chem.* **1987**, *91* (10), 2460.

(9) (a) Wiley, W. C.; McLaren, I. H. *Rev. Sci. Instrum* **1955**, *26* (12), 1150. (b) Poschenrieder, W. P. *Int. J. Mass Spectrom. Ion Phys.* **1972**, *9*, 357.

(10) (a) Bahatt, D.; Even, U.; Levine, R. D. *J. Chem. Chem.* **1993**, *98* (2), 1. (b) Bahatt, D.; Cheshnovsky, O.; Even, U. Submitted to *Z. Phys. Chem.*

(11) Daley, N. R. *Rev. Sci. Instrum.* **1960**, *31*, 264.

(12) (a) Penner, A.; Amirav, A. Submitted to *J. Chem. Phys.* (b) Shalev, E.; Ben-Horin, N.; Even, U.; Jortner, J. *J. Chem. Phys.* **1991**, *95* (5), 3147.

(13) Meijer, G.; Berden, G.; Meerts, W. L.; Hunziker, H. E.; De-Vries, M. S.; Wendt, H. R. *Chem. Phys.* **1992**, *163*, 209.

(14) Siebrand, W. *The triplet state*; Cambridge University Press: New York; 1967; Vol. 31.

(15) (a) Ben-Horin, N.; Even, U.; Jortner, J. *J. Molec. Struct.* **1992**, *266*, 75. (b) Heidenreich, A.; Jortner, J. *Z. Phys. D*, in press.

(16) Katz, B.; Birth, M.; Jortner, J. *J. Chem. Phys.* **1969**, *50*, 5195.

(17) Gedanken, A.; Raz, B.; Jortner, J. *J. Chem. Phys.* **1973**, *58*, 1178.

(18) Dressler, K. *J. Chem. Phys.* **1961**, *35*, 165.

(19) Klein, M. L.; Venables, J. A. *Rare Gas Solids*; Academic Press: New York, 1976; p 387.

(20) Yokozeki, A.; Kuchitsu, K. *Bull. Chem. Soc. Jpn.* **1971**, *44*, 72.